



Influence of ground anchors corrosion and uncertainty strength parameters: A case study slope failure in northern Taiwan

An-Jui Li, Hsiu-Chen Wen, Varian Harwin Batistuta, Shih-Hao Cheng

[Outline]

Ground anchor corrosion and uncertainty in strength parameters, primary factors in slope failures

2010 incident on Freeway No. 3 in northern Taiwan.

Combined use of numerical modeling and random field approach to better understand influence of these factors on slope stability.

[Methods]

Universal Distinct Element Code (UDEC) to perform numerical simulations, which considered ground anchor corrosion, discontinuity analysis, and the random field of strength parameters.

Back-analysis of original slope design using both uniform and random field models to assess influence of spatial variability on slope stability.

[Results]

Ultimate tensile strength ( $T_{max}$ ) of ground anchors significantly impacts slope stability, with anchor failure starting to occur when  $T_{max}$  is reduced below 70 tons, leading to slope failure.

Fs decreased from 1.44 to as low as 0.99 when considering anchor corrosion and residual strength parameters.



Fig. 1. Site photograph (a) Freeway No.3 landslide in Taiwan; (b) Corroded ground anchors from the field investigation (provided by Dr. Cheng).

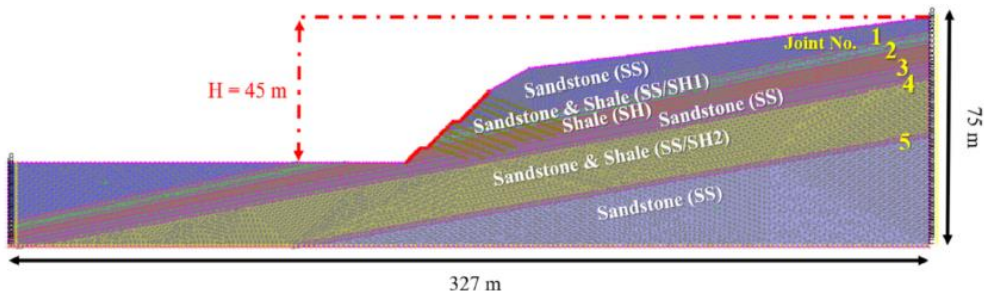


Fig. 2. Geological profile of a cross-section and slope geometry dimension of the slope on Freeway No.3.

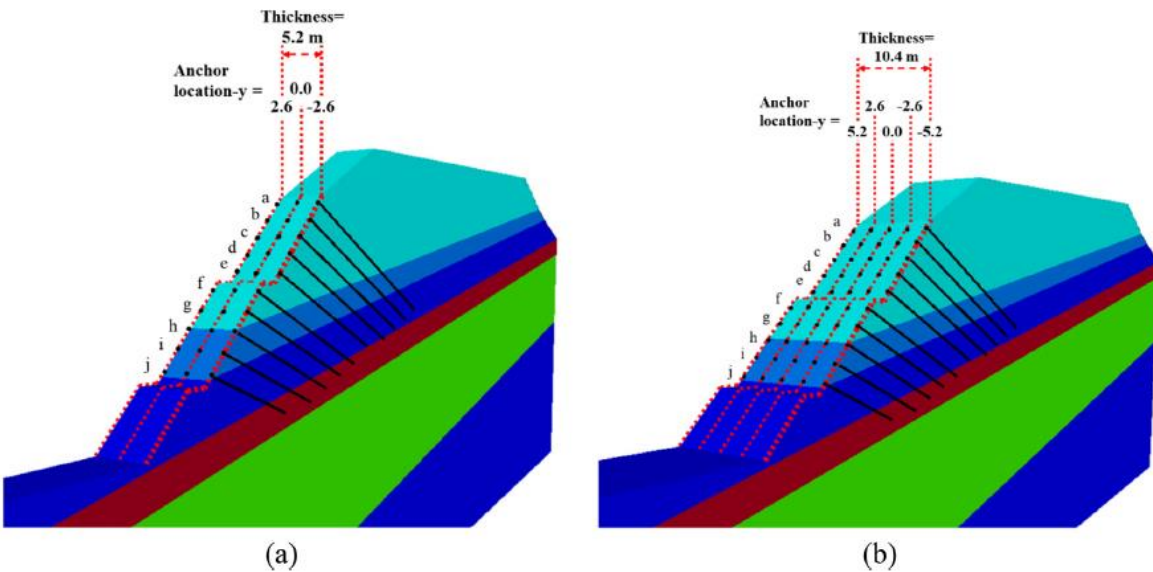


Fig. 8. 3D slope models (a) 3-column ground anchors (b) 5-column ground anchors.

[Outline]

Traditional bearing capacity formulas for strip footings do not adequately account for ultimate tensile capacity of soils

Modified formula incorporates ultimate tensile strength of soil.

[Methods]

Theoretical analysis and numerical simulations.

Modified bearing capacity formula by integrating ultimate tensile capacity into classical bearing capacity equations.

Numerical simulations were then conducted to validate modified formula against existing experimental data and to assess its accuracy under various soil conditions.

[Results]

Modified formula improves the prediction accuracy of the bearing capacity of strip footings.

Specifically, ultimate bearing capacity predictions were within 5% of the observed values from experimental data, compared to deviations of up to 20% using traditional formulas.

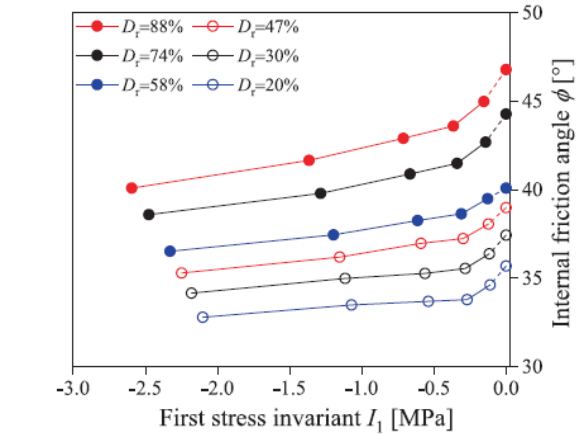


Fig. 1. Relationship between internal friction angle and first stress invariant for Toyoura sand (after Tatsuoka et al. (1986)).

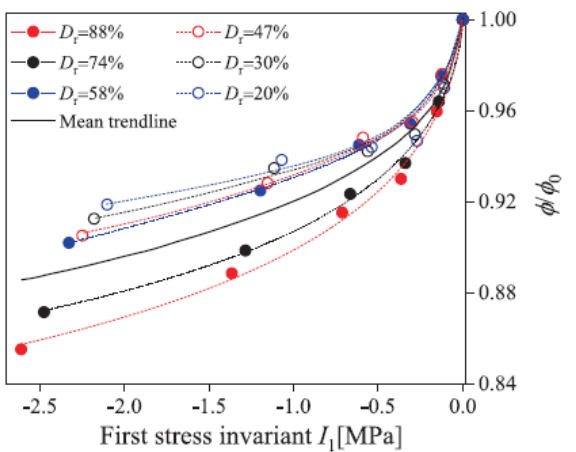


Fig. 2. Normalized relationship between  $\phi/\phi_0$  and  $I_1$  for Toyoura sand.

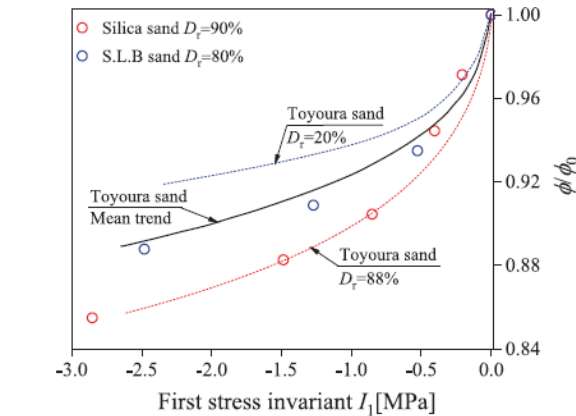


Fig. 3. Comparison of normalized relationship between  $\phi/\phi_0$  and  $I_1$  for various sandy soils.

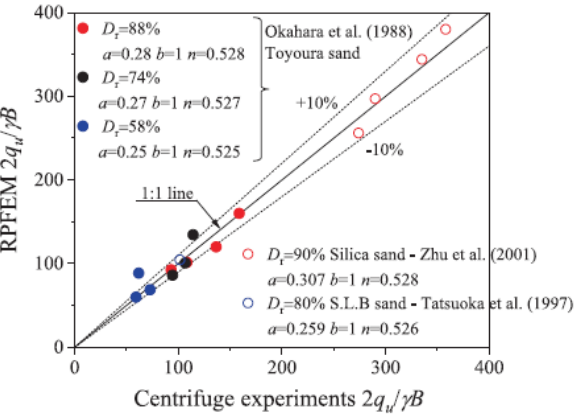


Fig. 4. Validation of analysis method for various sandy soils in cases of  $B$  up to 4 m.

Soils and Foundations 63 (2023) 101294

My road in search of elastoplastic soil mechanics

<https://doi.org/10.1016/j.sandf.2023.101294>

Akira Asaoka

New analytical method for predicting stresses around rectangular tunnels under arbitrary stress boundary conditions

Ping Wu, Xuejun Sun, Gang Chen, D.Y. Zhu, Shuanglong Tao, Lin Qin, Lei Wang, Xiangsheng Chen

[Outline]

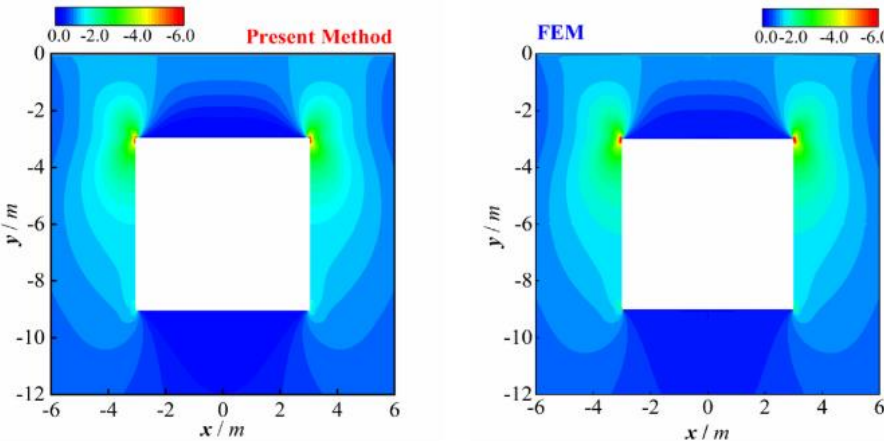
New analytical method for predicting stresses around rectangular tunnels.  
{accurate stress prediction by considering initial stress state and support pressures}

[Methods]

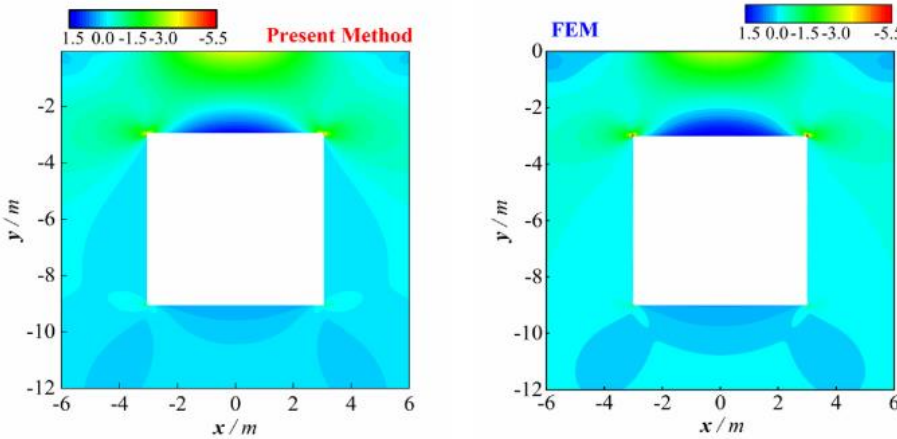
Model 1 half-plane without tunnel {calculated using existing analytical solutions}  
Model 2 half-plane with tunnel {involved applying virtual tractions and using an efficient iterative procedure to determine the stresses}

Results

High stress concentrations at the four corners of rectangular tunnels.  
When tunnel's burial depth was 10 times its height, the stress state was unchanged from initial state before excavation.  
for aspect ratios between 1.0 and 5.0, tensile stresses occurred on tunnel roof and floor, while compressive stresses were observed on the side walls



(a)



(b)

Fig. 9. Comparisons of stress fields around the tunnel under surcharge loads between the presented method and FEM: (a) stress  $\sigma_y$ ; (b) stress  $\sigma_x$ .



Observation of soil-structure interaction in double sheet pile method using X-ray CT

Hideharu Sugimoto, Shunsuke Akagi, Ayaka Nasu, Hideki Nagatani, Takahiro Sato, Toshifumi Mukunoki, Jun Otani

[Outline]

Interaction between soil and the double sheet pile method crucial for improving the displacement control and load-bearing capacity in construction.

Examining effects of friction between sheet piles and soil.

By using X-ray CT imaging, study seeks to visualize and analyze inner soil and sheet piles behavior during excavation and loading.

[Methods]

Model tests + industrial X-ray CT

- 1. polycarbonate sheet piles without sand attachment (Case Low S.R.)
- 2. Increased friction by coating the sheet piles with Toyoura sand (Case High S.R.).

[Results]

Increasing friction between sheet piles and inner soil resulted in a 25% increase in overall stiffness and changed the load-displacement trend.

In Case High S.R., where friction was increased, inner soil deformed significantly, and no slippage occurred at the boundary between sheet piles and inner soil, indicating integrated behavior.

In Case Low S.R., slippage occurred at the boundary, and inner soil and sheet piles behaved separately

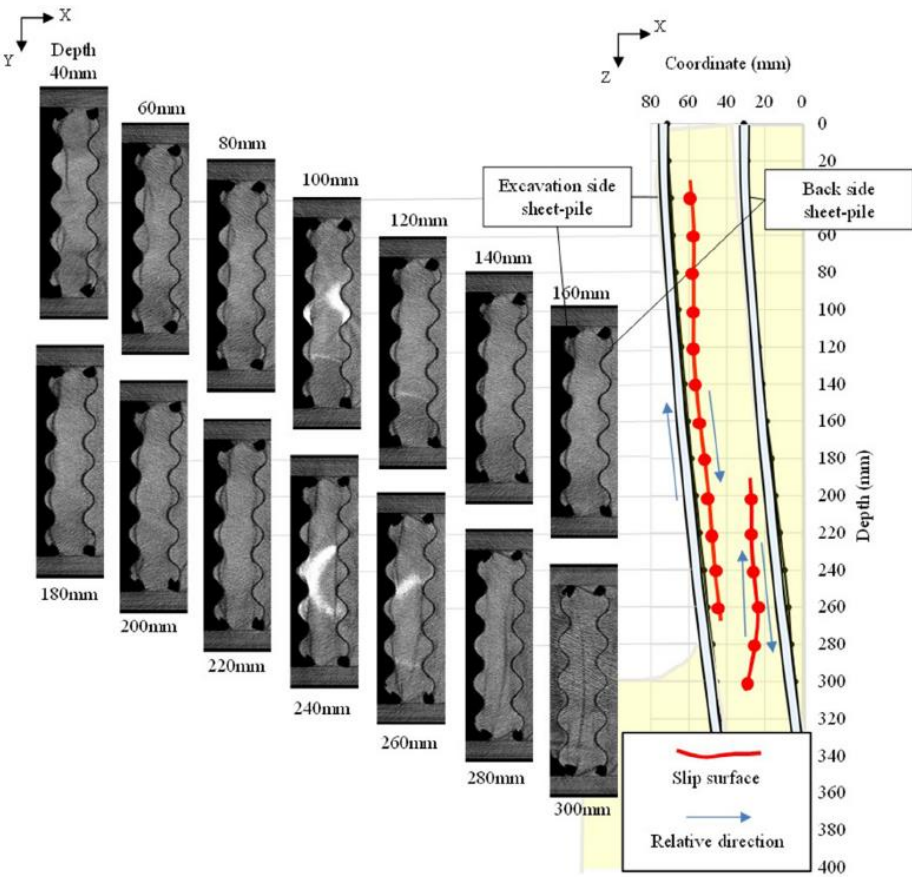


Fig. 18. Assumed slip line in inner soil of Case High S.R.

Research on the improvement of rainfall infiltration behavior of expansive soil slope by the protection of polymer waterproof coating

Shaokun Ma, Min Ma, Zhen Huang, Yu Huc, Yu Shao

[Outline]

Rainfall infiltration in slopes - lead to severe instability and landslides.  
Improve infiltration behavior of slopes by using a polymer waterproof coating to reduce water infiltration and increase slope stability.

[Methods]

Experiments to simulate rainfall on soil with and without polymer waterproof coating.  
Permeability tests, infiltration rate measurements, and stability analysis  
Compare the infiltration rates and stability of treated versus untreated soil samples under controlled conditions.

[Results]

**Infiltration Rate Reduction:** Polymer coating significantly reduced the infiltration rate by 50%, from 0.04 cm/min to 0.02 cm/min.  
**Increased Stability:** Slope stability improved, with a reduction in the factor of safety from 1.2 to 1.8 when the coating was applied.  
**Enhanced Soil Properties:** Permeability decreased from  $1 \times 10^{-5}$  cm/s to  $1 \times 10^{-7}$  cm/s, indicating a substantial improvement in water resistance.

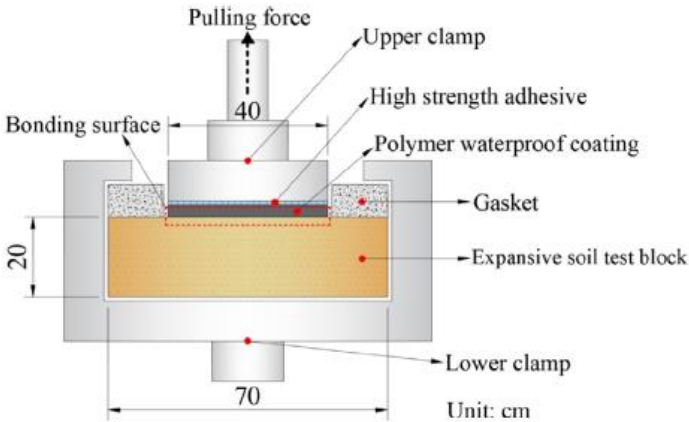


Fig. 5. Schematic diagram of the assembly of expansive soil test block and tensile equipment.

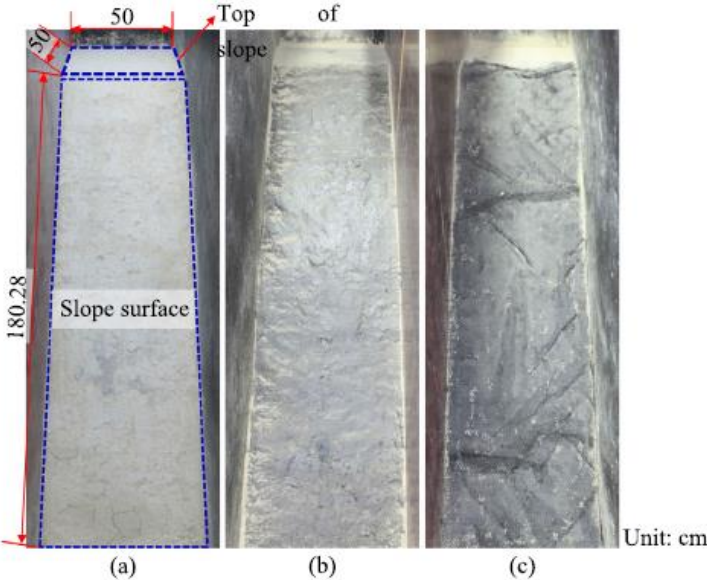


Fig. 11. Expansive soil slope model: (a) Slope I; (b) Slope II; (c) Slope III.